Facile and reversible double dearomatization of pyridines in non-phosphine MnI complexes with N,S-donor pyridinophane ligand

doi: info:doi/10.1039/C9CC00424F

Journal Name

COMMUNICATION

Facile and reversible double dearomatization of pyridines in non-phosphine Mn^{I} complexes with N,S-donor pyridinophane ligand†

Received 00th January 20xx,
Accepted 00th January 20xx

DOI: 10.1039/x0xx00000x

www.rsc.org/

Abir Sarbajna,[#a] Pradnya H. Patil,[#a] Minh Hoan Dinh,[a] Olga Gladkovskaya,[a] Robert R. Fayzullin,[b] Sébastien Lapointe,[a] Eugene Khaskin[a] and Julia R. Khusnutdinova*[a]

Single and double dearomatization of pyridine rings was observed in Mn^{I} complexes with an N2S2 pyridinophane ligand via deprotonation of one or two CH_2 arms, respectively. In contrast to other N,S-donor pincer-like systems, the dearomatized (N2S2)Mn species were found to be stable, with the dearomatization being reversible.

Metal-Ligand Cooperation (MLC) has been identified as a key tool for the activation and conversion of ubiquitous small molecules into value–added chemicals, fuels and feedstocks.[1] Relying on the design principles of many naturally occurring enzymes,[2] the concept of MLC implies that both the metal and the ligand take part in the bond activation step, where the overall oxidation number of the metal remains unchanged, providing a low energy pathway for many chemical processes.[1d, 1e]

Pyridine-based pincer complexes, mainly with phosphine-donor arms, have emerged as capable catalysts for small molecule activation owing to ligand participation in the activation of H-X bonds (X = H or heteroatom).[3] Deprotonation of the methylene group on one of the arms of such a pyridine–based pincer complex can lead to the formation of a dearomatized species, which can heterolytically cleave inert bonds, with the thermodynamic driving force being re-aromatization of the pyridine ring (Scheme 1).[4]

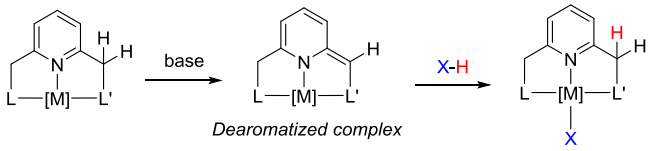

Scheme 1 Dearomatization of pyridine-based pincer ligands, followed by aromatization with the concomitant activation of chemical bonds (X–H; X=H, C, O, N). L and L' are ligating groups.

Preserving oxidation state of the metal during bond activation enabled by MLC is crucial for catalysis by earth-abundant metals, in particular Mn^{I}, for which the importance of the Mn^{I} oxidation state has been highlighted in catalytic hydrogenation.[5] The majority of the current examples of Mn^{I}-catalyzed hydrogenation/dehydrogenation reactions involve phosphine-based ligands.[5a, 6] The presence of phosphine atoms in PNN or PNP ligands associated with MLC means that they are extremely air and moisture sensitive, and are often synthetically challenging and expensive. With the recent surge of interest in catalysis by earth-abundant Mn,[5a, 6] developing inexpensive and readily available non-phosphine ligands would provide immediate economic benefits. Indeed, recently there has been a raising number of studies showing that transition metal complexes N,S-donor ligands often show outstanding efficiency and low temperature reactivity in catalysis.[7] Utilization of S-donor analogs may provide significant advantages compared to phosphines, such as synthetic availability on large scale, low cost and higher air stability.[7] However, there is a paucity of detailed reports on MLC reactivity in N,S-donor pincer ligand.

In this work, we demonstrate that manganese complexes supported by a macrocyclic 2,11-dithia[3.3](2,6)pyridinophane (N2S2) ligand exhibit fully reversible and fast single and double deprotonation of the methylene arms, leading to dearomatization of one or two pyridine rings. Such reactivity with sulfide-donor pyridine-based ligands has not, to the best of our knowledge, been reported previously.

Mechanistic studies on N,S donor ligand mediated catalysis are complicated by undesired side-reactions, lack of reversibility, and low stability of the reactive species. For example, Milstein et al. have demonstrated that dearomatized Ru complexes of sulfide-based PNS type ligands undergo spontaneous dimerization via C–S bond cleavage, resulting in the loss of an S-bound ^{t}Bu group and catalyst deactivation.[8] On the other hand, dearomatized Rh complex derived from

[a] Coordination Chemistry and Catalysis Unit, Okinawa Institute of Science and Technology Graduate University, 1919-1 Tancha, Onna-son, Kunigami-gun, Okinawa 904-0495, Japan
[b] Arbuzov Institute of Organic and Physical Chemistry, FRC Kazan Scientific Center, Russian Academy of Sciences, 8 Arbuzov Street, Kazan 420088, Russian Federation
# These authors made equal contributions.

† Electronic supplemental information (ESI) available: experimental procedures and characterization data. CCDC 1887964-1887968. For ESI and crystallographic data in CIF or other electronic format see DOI: 10.1039/x0xx00000x

sulfoxide-based NNS pincer ligands was resistant towards reprotonation even in the presence of excess protic solvent.[9] Thus, for sulfur-donor ligands it is thus crucial to find a balance between stability and the ability to undergo reversible deprotonation in order to enable MLC reactivity.

In this work, we take advantage of the macrocyclic structure and high stability of N2S2 pyridinophane, which renders the associated Mn^{I} complexes remarkably stable and allows their structural and spectroscopic characterization. The accessibility and reversible formation of the three different forms, doubly dearomatized, singly dearomatized, and fully aromatized species $[(N2S2)Mn(CO)_2]^+$, suggest the potential use of these simple ligands for new types of small molecule activation. Interestingly, the mono-dearomatized species persists even in the presence of an excess water.

To obtain a Mn^{I} precursor with the neutral N2S2 ligand, $Mn(CO)_5Br$ was reacted with 1 equivalent of ligand in a toluene/methanol mixture at 80 °C to produce the yellow colored cationic compound $[Mn(CO)_2(N2S2)]Br$ (**[1]Br**) in 95% yield. The X-ray structure shows a distorted octahedral Mn center with the N2S2 ligand bound in a *syn*-boat-boat conformation (Fig. 1). The stretching bands of carbonyl ligands in the solid-state FT-IR spectrum appear at 1934 and 1866 cm^{-1}. The solution NMR spectrum is consistent with a symmetrical structure showing aromatic pyridine *meta*- and *para*- protons at 7.47 and 7.74 ppm, respectively, along with two geminally coupled doublets of CH_2 groups at 4.79 and 4.90 ppm.

Deprotonation of **[1]Br** with 2.2 equivalents of ^{t}BuOK in THF-d_8 led to the formation of an orange solution within a few seconds, which was characterized by NMR spectroscopy (vide infra). Filtration of the THF solution and crystallization by pentane vapor diffusion at –30°C produced orange crystals of the doubly dearomatized anionic complex $[K(THF)_3][(N2S2^{**})Mn(CO)_2]$ (**2**) (Scheme 2; N2S2** denotes a doubly dearomatized ligand). Complex **2** was stable for several hours in the solid state and several weeks in solution at -30 °C.

X-ray diffraction data revealed that compound **2** in the crystalline state represents a 1D polymeric structure (Fig. S50 in ESI†) formed along the shortest axis 0*a* by means of cation (K^+)…π(N2S2**) interactions and coordination bonds between the potassium and one of two carbonyl oxygen atoms of the anionic complex (K1–O1 is 2.733(2) Å). The distances of cation K1 to the plane and the centroid Py(1) (pyridine ring containing N1 atom) are 2.9754(14) Å and 3.0233(13) Å [symmetry operation (*x*–1, *y*, *z*)], while the distances of K1 to the plane and the centroid of Py(2) are longer and equal to 3.113(2) Å and 3.4968(13) Å, respectively. The bonds C16–C17 and C21–C22 are of 1.499(4) and 1.508(4) Å, which in close agreement with a typical $C(sp^2)$–$C(sp^3)$ bond length (*ca.* 1.51 Å), whereas C11–C12 and C26–C27 are significantly shorter and equal to 1.384(4) and 1.367(4) Å (for comparison a double carbon bond length is *ca.* 1.34 Å), implying that deprotonation has occurred at both C11 and C27 centres (Fig. 1). The positions of the hydrogen atom H11 and H27 of the deprotonated arms were determined by difference Fourier maps. As expected, the sulfur-carbon bonds S1–C11 and S2–C27 (1.737(3) and 1.752(3) Å) on the deprotonated arms become meaningfully shorter compared to S1–C21 and S2–C17 (1.820(3) and 1.825(3) Å). At the same time redistribution of bond lengths of both nitrogen heterocycles corresponds with dearomatization of the pyridine moieties. More significant shortening of the corresponding carbon bonds (Δ ≈ 0.13 Å) comparing with sulfur-carbon bonds (Δ ≈ 0.08 Å) suggests that the resonance form with dearomatized pyridine ring contributes more to charge delocalization than that of the sulfur ylide, at least in the solid state. No noteworthy changes of coordination bond lengths occur at the Mn center upon formation of **2** from **[1]Br**.

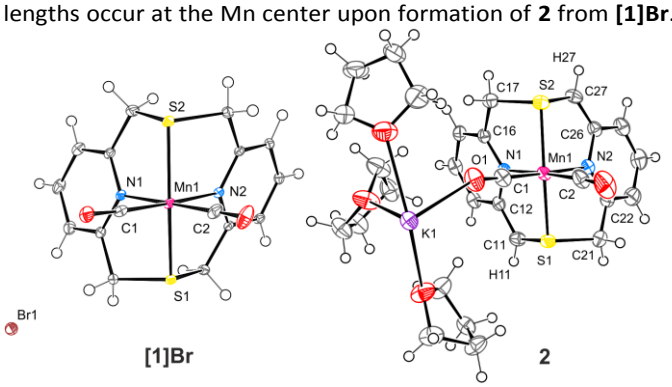

Fig. 1 ORTEP of complex **[1]Br** and the asymmetric unit of doubly dearomatized complex **2** at 50% probability level of non-hydrogen atoms. Minor disordered components of THF ligands are omitted for clarity.

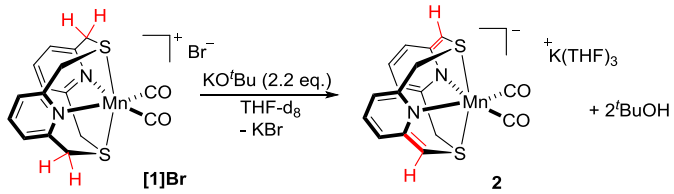

Scheme 2 Double deprotonation/dearomatization of complex **[1]Br**.

The characteristic changes indicative of dearomatization of both pyridine rings were also observed in the NMR spectrum. Thus, ^{1}H NMR in THF-d_8 displays a significant upfield shift of the pyridine protons which appear as a doublet of doublets at 6.13 ppm for the proton in *para* position with respect to the N atom (verified by appropriate cross peaks in COSY spectra) and two doublets at 5.74 and 5.37 ppm for the two *meta* protons. The CH protons of the deprotonated arms appear as a sharp singlet at 3.38 ppm, whereas the the two protons on the remaining non-deprotonated arms appear as two geminally coupled doublets at 3.44 ppm. The solid-state FT-IR spectrum shows the shifting of the carbonyl peaks to 1893 and 1803 cm^{-1}, indicative of stronger π-backdonation to carbonyls from more electron-rich Mn^{I} centre supported by two negatively charged amide donors of dearomatized pyridine groups.

Once we had fully characterized **2**, we were interested in seeing whether the deprotonation was reversible. Indeed, when adding 2.5 equivalents of HBr or HCl in diethyl ether to the *in situ* generated **2**, a new product that was identified as **[1]Br** or **[1]Cl**, respectively, was formed. X-ray structures, (Fig. 2) as well as spectroscopic features of **[1]Br** and **[1]Cl** are very

similar. Reversibility between dearomatized and aromatized forms could also be achieved by the addition of a weak acid. Addition of 3.5 equivalents of formic acid to **2** leads to the formation of a formate counterion complex **[1]HCOO**, in which a formate counterion is hydrogen bonded to another HCOOH molecule (Fig. 2). Both the newly isolated **[1]Cl** and **[1]HCOO** can be deprotonated with 2.2 equivalents of KO^{t}Bu to reform **2**, demonstrating repeatable reversibility between the dearomatized and aromatized complexes.

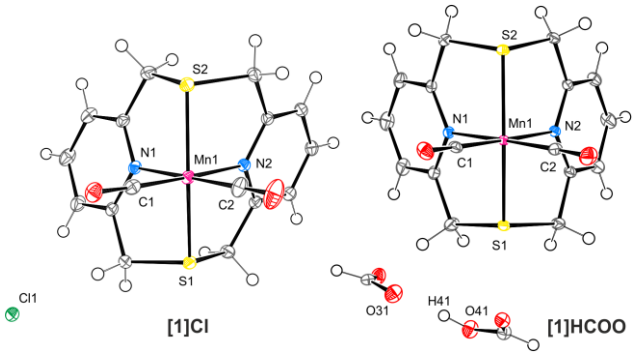

Fig. 2 ORTEP of complexes **[1]Cl** and **[1]HCOO** at 50% probability level of non-hydrogen atoms.

We next attempted to find the "missing link", or the monodeprotonated N2S2 ligand (N2S2*) complex. However, despite repeated attempts, we could not isolate the compound by adding 1.2-1.8 equivalents of KO^{t}Bu to **[1]X** (X = Br, Cl, HCOO). Instead, in all cases incomplete conversion to complex **2** was observed. Interestingly, when we added one equivalent of an acid (HBr, HCl or HCOOH) to the doubly dearomatized compound **2**, an orange-coloured neutral compound [(N2S2*)Mn(CO)$_2$], **3**, was obtained. ^{1}H NMR confirmed the deprotonation of only one of the arms and displayed six sets of doublets for the three methylene groups and one singlet for the dearomatized CH group at 3.54 ppm. DEPT-135 NMR analysis proved that the peak at 64.6 ppm corresponds to the deprotonated carbon arm, whereas the three peaks at 60.1, 52.2 and 47.5 ppm, which are reversed in phase, are due to the three CH_2 groups. The aromatic region exhibits six signals covering the range from 7.55 to 5.63 ppm for aromatic pyridine and dearomatized pyridine fragments consistent with an unsymmetrical mono-dearomatized structure. Stretching frequencies at 1918 and 1834 cm^{-1} (solid state) for the carbonyls are indicative of an intermediate degree of π-backdonation, putting the new complex on the expected **[1]Br** < **3** < **2** trendline.

X-ray diffraction analysis of **3** confirms the absence of counter ions. However, the structure is CH_2/CH disordered (Fig. 3) into two components with the same occupancies. The apparent geometry of the ligand appeared to be averaged over two forms with either C11 or C27 arm being deprotonated. Nevertheless, the overall bond lengths of C11–C12 and C26–C27 are equal to *ca.* 1.44 Å, which is shorter than that of C16–C17 and C21–C22 (*ca.* 1.50 Å). The overall sulfur-carbon bonds S1–C11 and S2–C27 (*ca.* 1.78 Å) in the deprotonated parts become shorter than that of S1–C21 and S2–C17 (*ca.* 1.82 Å) as well. Bond length alternation in the nitrogen heterocycles agrees with dearomatization of the pyridine moiety of each disordered component.

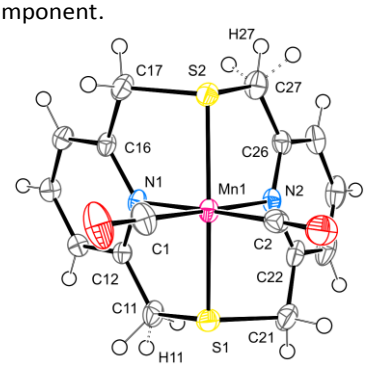

Fig. 3 ORTEP of mono-deprotonated complex **3** at 50% probability level of non-hydrogen atoms. The second disordered component is shown by dashed lines.

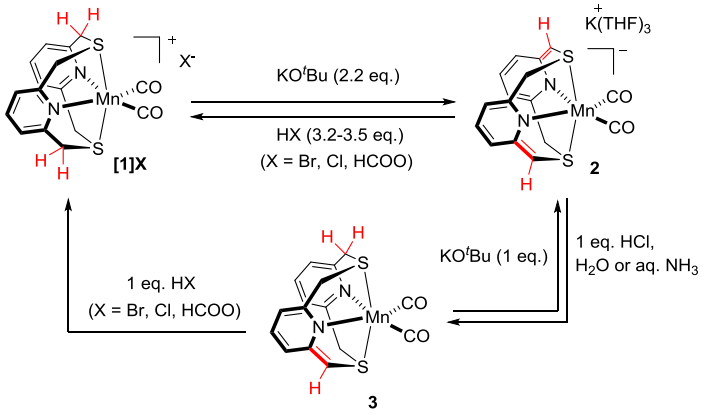

Scheme 3 Interconversions between **[1]X** (X = Br, Cl, HCOO), **2** and **3**

Compound **3** could be deprotonated by only one equivalent of KO^{t}Bu to yield **2**. Conversely, **3** could be protonated by adding one more equivalent of an acid HX (X = Br, Cl, HCOO) to form **[1]X** (X = Br, Cl, HCOO) with the appropriate counterion. These transformations show that deprotonation and dearomatization of the N2S2-supported Mn complexes is indeed reversible and all three observed forms of these complexes supported by neutral, mono-deprotonated and doubly deprotonated N2S2 ligand are stable under the reaction conditions (Scheme 3). Therefore, by contrast to the pincer-based systems, pyridinophane N2S2 allows for the stabilization of dearomatized species and for an exploration of their reactivity.

Accordingly, we examined the reactivity of the doubly deprotonated complex **2** in the activation of weakly acidic proton donors. Gratifyingly, we saw that the addition of one equiv. of H_2O to **2** led to the clean formation of **3**. Moreover, even after the addition of >10 equivalents of water, only **3** could be detected (see ESI†). The transformation of **2** to **3** could also be achieved using one equiv. of aqueous ammonia solution to simulate a weakly basic media. Several deuteration

studies were carried out to probe the reversibility of substrate activation. When 15 equivalents of DBr was added to **2**, ^{2}H NMR showed two peaks at 4.99 and 4.78 ppm indicating that D incorporation occurs in a non-stereoselective manner at both protons of methylene arms. The decrease in CH_2 integration showed that 67% D incorporation had taken place, greater than that expected from incorporation of only two deuterium atoms and indicative of reversible nature of this process. At the same time, no further deuterium incorporation was observed when isolated complexes **[1]Br** or **[1]HCOO** were reacted with excess DBr or HCOOD, respectively. In a similar experiment with DCl and HCOOD, 57-61% D incorporation was observed. Interestingly, when D_2O (3 equivalents) was used as a reagent for deuteration, partially deuterated **3** was obtained with D incorporated in all CH and CH_2 positions, showing that H/D exchange is reversible. Although complex **2** did not show catalytic reactivity in direct or transfer hydrogenation of ketones or dehydrogenation of alcohols likely due to the presence of two strongly bound CO ligands, studies are currently underway to create more labile systems in which coordination site at the metal would be available to enable true metal-ligand cooperative reactivity.

In summary, we obtained and characterized manganese(I) complexes supported by 2,11-dithia[3.3](2,6)pyridinophane ligand in its neutral, mono-deprotonated, and the unusual doubly deprotonated states. The stability of these N,S-donor ligated complexes is likely due to macrocyclic nature of the pyridinophane ligand. Although this ligand resembles previously studied sulfur-based pincer ligands, by contrast to the previous systems, no ligand decomposition or fragmentation was observed in the case of N2S2 complexes. Single and double dearomatization of the pyridine rings that occurs upon deprotonation is evident from NMR and X-ray diffraction analyses, while minor contribution from sulfur ylide form is suggested from bond length analysis. Moreover, in contrast to previous systems, all transformations between the three different forms are reversible, with the degree of reversibility determined by the acidity of the reaction mixture.

In conclusion, this study presents a model system that can serve as an example for the potential of MLC reactivity in non-phosphine, sulfur-based ligands. Our current research efforts will be directed to application of such reactivity for small molecule activation using simple and readily accessible N,S-donor ligands.

The authors would like to thank Dr. Michael Roy for HRMS analysis and acknowledge Okinawa Institute of Science and Technology Graduate University for start-up funding.

Conflicts of interest

The authors declare no conflicts of interest.

Notes and references

1. *(a)* R. Noyori, M. Yamakawa and S. Hashiguchi, *J. Org. Chem.*, 2001, **66**, 7931-7944; *(b)* H. Grützmacher, *Angew. Chem. Int. Ed.*, 2008, **47**, 1814-1818; *(c)* T. Ikariya and M. Shibasaki, in *Bifunctional Molecular Catalysis*, Springer, 2011; *(d)* J. I. van der Vlugt, *Eur. J. Inorg. Chem.*, 2012, 363-375; *(e)* J. R. Khusnutdinova and D. Milstein, *Angew. Chem. Int. Ed.*, 2015, **54**, 12236-12273; *(f)* P. A. Dub and J. C. Gordon, *ACS Catal.*, 2017, **7**, 6635-6655.
2. *(a)* H.-J. Fan and M. B. Hall, *J. Am. Chem. Soc.*, 2001, **123**, 3828-3829; *(b)* D. J. Evans and C. J. Pickett, *Chem. Soc. Rev.*, 2003, **32**, 268-275.
3. *(a)* C. Gunanathan and D. Milstein, *Acc. Chem. Res.*, 2011, **44**, 588-602; *(b)* C. Gunanathan and D. Milstein, *Chem. Rev.*, 2014, **114**, 12024-12087; *(c)* E. Balaraman and D. Milstein, in *Ruthenium in Catalysis*, eds. P. H. Dixneuf and C. Bruneau, Springer International Publishing, Cham, 2014, pp. 19-43; *(d)* C. Gunanathan and D. Milstein, *Science*, 2013, **341**, 1229712.
4. V. T. Annibale and D. Song, *RSC Adv.*, 2013, **3**, 11432-11449.
5. *(a)* F. Kallmeier, T. Irrgang, T. Dietel and R. Kempe, *Angew. Chem. Int. Ed.*, 2016, **55**, 11806-11809; *(b)* A. Dubey, L. Nencini, R. R. Fayzullin, C. Nervi and J. R. Khusnutdinova, *ACS Catal.*, 2017, **7**, 3864-3868.
6. *(a)* S. Elangovan, M. Garbe, H. Jiao, A. Spannenberg, K. Junge and M. Beller, *Angew. Chem. Int. Ed.*, 2016, **55**, 15364-15368; *(b)* S. Elangovan, C. Topf, S. Fischer, H. Jiao, A. Spannenberg, W. Baumann, R. Ludwig, K. Junge and M. Beller, *J. Am. Chem. Soc.*, 2016, **138**, 8809-8814; *(c)* A. Nerush, M. Vogt, U. Gellrich, G. Leitus, Y. Ben-David and D. Milstein, *J. Am. Chem. Soc.*, 2016, **138**, 6985-6997; *(d)* M. B. Widegren, G. J. Harkness, A. M. Z. Slawin, D. B. Cordes and M. L. Clarke, *Angew. Chem. Int. Ed.*, 2017, **56**, 5825-5828; *(e)* A. Mukherjee, A. Nerush, G. Leitus, L. J. W. Shimon, Y. Ben David, N. A. Espinosa Jalapa and D. Milstein, *J. Am. Chem. Soc.*, 2016, **138**, 4298-4301; *(f)* R. van Putten, E. A. Uslamin, M. Garbe, C. Liu, A. Gonzalez-de-Castro, M. Lutz, K. Junge, E. J. M. Hensen, M. Beller, L. Lefort and E. A. Pidko, *Angew. Chem. Int. Ed.*, 2017, **56**, 7531-7534; *(g)* A. Mukherjee and D. Milstein, *ACS Catal.*, 2018, **8**, 11435-11469; *(h)* Y.-Q. Zou, S. Chakraborty, A. Nerush, D. Oren, Y. Diskin-Posner, Y. Ben-David and D. Milstein, *ACS Catal.*, 2018, **8**, 8014-8019; *(i)* T. Zell and R. Langer, *ChemCatChem*, 2018, **10**, 1930-1940; *(j)* G. A. Filonenko, R. van Putten, E. J. M. Hensen and E. A. Pidko, *Chem. Soc. Rev.*, 2018, **47**, 1459-1483; *(k)* N. Gorgas and K. Kirchner, *Acc. Chem. Res.*, 2018, **51**, 1558-1569; *(l)* F. Kallmeier and R. Kempe, *Angew. Chem. Int. Ed.*, 2018, **57**, 46-60.
7. *(a)* Y. Morisaki, T. Ishida and Y. Chujo, *Org. Lett.*, 2006, **8**, 1029-1032; *(b)* D. Spasyuk, S. Smith and D. G. Gusev, *Angew. Chem. Int. Ed.*, 2013, **52**, 2538-2542; *(c)* R. Patchett, I. Magpantay, L. Saudan, C. Schotes, A. Mezzetti and F. Santoro, *Angew. Chem. Int. Ed.*, 2013, **52**, 10352-10355; *(d)* P. A. Dub, B. L. Scott and J. C. Gordon, *Organometallics*, 2015, **34**, 4464-4479; *(e)* B. M. Trost and M. Rao, *Angew. Chem. Int. Ed.*, 2015, **54**, 5026-5043; *(f)* P. Puylaert, R. van Heck, Y. Fan, A. Spannenberg, W. Baumann, M. Beller, J. Medlock, W. Bonrath, L. Lefort, S. Hinze and J. G. de Vries, *Chem. Eur. J.*, 2017, **23**, 8473-8481; *(g)* B. M. Stadler, P. Puylaert, J. Diekamp, R. van Heck, Y. Fan, A. Spannenberg, S. Hinze and J. G. de Vries, *Adv. Synth. Catal.*, 2018, **360**, 1151-1158.
8. M. Gargir, Y. Ben-David, G. Leitus, Y. Diskin-Posner, L. J. W. Shimon and D. Milstein, *Organometallics*, 2012, **31**, 6207-6214.
9. T. Schaub, U. Radius, Y. Diskin-Posner, G. Leitus, L. J. W. Shimon and D. Milstein, *Organometallics*, 2008, **27**, 1892-1901.

